AD NUMBER
AD394828
CLASSIFICATION CHANGES
TO: unclassified
FROM: confidential
LIMITATION CHANGES
TO: Approved for public release, distribution unlimited
FROM: Distribution: Controlled: all requests to Director, Naval Research Lab., Washington, D. C. 20390.
AUTHORITY
NRL ltr, 21 Nov 2002; NRL ltr, 21 Nov 2002

394 828

SECRET

NRL Memorandum Report 1927

Copy No. 19 of 75 Copies

Summary Report
Continuation of
Experimental Study of Small Particle Impacts Into Ablative Materials

[Unclassified Title]

S. M. HALPERSON

Sponsored By
Advanced Research Projects Agency
Strategic Technology Office

"This document contains information affecting the National Defense of the United States within the meaning of the Espionage Laws, Title, 18, U. S. C., Section 795 and 794. Its transmission or the revelation of its contents in any manner to an unauthorized person is prohibited by law."

July 1968

STATEMENT #5 CLASSIFIED

In addition to security requirements which apply to this document and must be met, it may be further distributed by the holder only with specific approval of ______________________

NAVAL RESEARCH LABORATORY
Washington, D.C. 20390

SECRET

DOWNGRADED AT 12 YEAR INTERVALS; NOT AUTOMATICALLY DECLASSIFIED. DOD DIR 5200.10

Downgraded at 12 year intervals; Not automatically declassified.

SEE INSIDE OF FRONT COVER FOR DISTRIBUTION RESTRICTIONS

SECURITY

This document contains information affecting the national defense of the United States within the meaning of the Espionage Laws, Title 18, U.S.C., Sections 793 and 794. The transmission or revelation of its contents in any manner to an unauthorized person is prohibited by law.

In addition to security requirements which apply to this document and must be met, it may be further distributed by the holder *only* with specific prior approval of the Director, Naval Research Laboratory, Washington, D.C. 20390.

UNCLASSIFIED

CONTENTS

UNCLASSIFIED

ABSTRACT (U)

(U) This report is a continuation of the work described in NRL Memorandum Report 1813, entitled "Experimental Study of Small Particle Impacts Into Ablative Materials".

(S) Utilizing the light-gas gun, impact tests with glass spheres from 3.18 mm to 100μ in diameter were made into three ablatives; phenolic nylon, carbon phenolic, and oblique tape wound refrasil. Velocities ranged from 0.74 to 7.9 km/sec and angles of obliquities ranged from 10° to 90°.

(S) It was established that modified explosive scaling does not hold true for hypervelocity impacts into ablatives, and dimensionless damage parameter such as penetration/projectile size are dependent on both velocity and projectile dimension rather than on velocity alone.

(S) Penetration measurements of virgin phenolic nylon targets impacted by 3.18-mm aluminum spheres showed good correlation with the theoretical formula of Walsh. It was also determined that for obliquity tests where the normal velocity component/target sound speed ≥ 1, the mass loss and depth of penetration are proportional to the normal velocity component for angles of obliquity down to twenty degrees.

(S) Impact experiments were made with 1/2" x 1/2" x 1/4" char-layer specimens of carbon phenolic and oblique tape wound refrasil at room temperature and elevated temperatures, at normal incidence, and obliquities of 45° and 10°. Specimen mass loss was measured, and it was ascertained that for room temperature tests C_N (impact energy/mass loss) tends to increase slightly with decreasing angles of obliquity. Experiments where char-layer surface temperatures were raised to approximately 1600°F showed an expected decrease in C_N.

PROBLEM STATUS

This is the final report on the problem.

AUTHORIZATION

NRL Problem F04-11A
ARPA Order No. 149 Amendment No. 11
Program Code 6E30

ARPA Order No. 149 Amendment No. 12
Program Code 7E30

LIST OF SYMBOLS

p.n.	:	Phenolic nylon
c.p.	:	Carbon Phenolic
o.t.w.r.	:	Oblique tape wound refrasil
D_S	:	Diameter of particle or spherical projectile
θ	:	Acute angle between target surface and trajectory
P	:	Depth of penetration
v	:	Impact velocity
ρ_p	:	Density of projectile material
ρ_t	:	Density of target material
C_t	:	Sound speed of target material
K	:	Coefficient in penetration equation.
α	:	Exponent in penetration equation
V_c	:	Crater volume
E	:	Impact energy
n	:	Number of particles striking a target
C_N	:	Energy necessary to remove one gram of target material
M_{LH}	:	Mass loss of target due to heating
M_{LI}	:	Mass loss of target due to impact
M_L	:	Total mass loss of target $= M_{LH} + M_{LI}$

EXPERIMENTAL STUDY OF SMALL PARTICLE IMPACTS INTO ABLATIVE MATERIALS (U)

INTRODUCTION (U)

(S) This report is primarily concerned with extension of the work described in NRL Memorandum Report 1813, Reference 1. The problem is to simulate, in the laboratory, impact damage inflicted on thermal protection systems of ballistic missile nose-cones by minute dust particles. Erosive effects due to environmental factors such as rain or ice in the atmosphere or dust particles in clouds produced by nuclear explosions have not been previously considered by ballistic missile designers. It is estimated that nuclear dust clouds contain particles in the order of 20μ in diameter which have a density of approximately 2.5 gm/cm^3, Reference 1. NRL has been specifically concerned with the small particle impact problem.

(U) The total damage to the protection system is dependent on a number of factors, many of which are interdependent. Encounter velocity, particle size, density, and trajectory with respect to the heat shield surface, environmental and thermal conditions at the heat shield surface, heat shield material and thickness are all contributing factors in evaluating the vulnerability of a R/V to dust particle impact.

(U) Impact tests have been completed at NRL with aluminum and glass spherical projectile projectiles ranging in size from 100 μ to 3.18 mm in diameter. The target materials were phenolic nylon (p.n.), carbon phenolic (c.p.), and oblique tape wound refrasil (o.t.w.r.). Measured impact velocities ranged from 0.74 to 7.9 km/sec. Appendix 1 is a compilation of pertinent test data obtained during this reporting period.

(U) A number of tests were conducted on specimens which had been pre-charred in a high temperature flame prior to impact. The specimens were at room temperature when impacted. This is a more realistic approximation to the actual situation than virgin material impacts, since impacts into virgin material occur only at the stagnation point or portions of the re-entry vehicle where the char has been removed by aerodynamic shear forces. Undoubtedly firing into a heated char-layer is a truer analog to an operational situation; towards this objective a small radiation heating facility has been built, and a limited amount of data has been acquired from heated char-layer target impacts.

(U) This report covers the following topics:

I. Instrumentation for small particle impact studies.

II. The effect of projectile size on impact damage.

III. Impact damage to virgin ablative materials.

IV. Impact damage to charred ablative materials.

I. INSTRUMENTATION FOR SMALL PARTICLE IMPACT STUDIES (U)

(U) All the terminal ballistic data reported were obtained with a 40-mm, 30-caliber light-gas gun; the range facility has been fully described in Reference 1.

A. Velocity Measuring Instrumentation (U)

(U) The velocity measuring system is similar to that described in Reference 1. Two Beckman and Whitley image converter cameras, Model 501, with associated instrumentation are used. Two camera stations are needed to provide sufficient information to determine projectile velocity. Camera no. 1 is a horizontally aligned camera which views the vertical plane; camera no. 2 is a vertically aligned camera which views the horizontal plane.

(U) The major difference between the current system and the previous system is in the triggering mode. For the microparticle studies, it was determined that placing a trigger plate (make-circuit) in the field of view of the first camera was more reliable than placing the trigger plate off camera and computing a camera time delay based on the expected velocity and the distance between switch and camera.

(U) In the current system, since the trigger is in the field of view, the first camera delay time is set at zero microseconds from triggering. The second camera is triggered by the first camera; the time delay is computed from the estimated velocity and the separation between the two camera stations.

(U) Figures 1a and 1b show three 400μ diameter spheres at stations no. 1 and no. 2; visible in the pictures are fiducial marks spaced 0.5 cm apart, and reference markers, 16.05 cm apart, which are spatial references at the stations. The cameras had exposure settings of 10 nanoseconds. Visible in Figure 1a is the trigger plate. Five spheres were launched, and the spray from a ball impact can also be seen in 1a. The timing trace for the round is shown in Figure 1c; the 5 μs marks are from a Tektronix type 180 time-mark generator.

B. Target Heating Instrumentation (U)

(U) A small radiation heating facility was built for the express purpose of heating the char-layer target specimens (1/2" x 1/2" x 1/4") during impact. A radiator was chosen because it has electromagnetic waves as its mode of transmission rather than a plasma-jet or an oxygen-acetylene torch which employs convection as the principal mode of heat transfer. The latter method would not be totally satisfactory since portions of the frangible char-layer would be removed by the gas flow, making it difficult to maintain char-layer integrity prior to impact.

(U) Figure 2 is the schematic for the target heating system currently in operation at the NRL Small Particle Facility. The main component in this system is a tungsten coil heater, 7/8" inside diameter x 7/8" long, obtained from R.W. Mathes Company. The heater is powered from the low voltage-high current side of a transformer. Seventy ampere coil currents have produced temperatures in ablative samples slightly in excess of 2000°F. Temperature is measured with chromel-alumel thermocouples whose outputs are monitored on a Mosely type 680 recorder. The heater is mounted in a porcelain reflector open at both ends allowing the projectiles to pass through the heating chamber and impact the heated target without striking the heater or reflector. Disadvantages of this scheme are heater degradation and the resultant tungsten oxides evident on coil, reflector and specimen even at ambient pressures as low as 7-mm Hg air. This reaction is minimized by flushing out the test chamber with helium and performing the test in a reduced pressure helium environment.

II. EFFECT OF PROJECTILE SIZE ON IMPACT DAMAGE (U)

(S) The effect of projectile size on impact damage is of extreme importance not only in this program but in other branches of hypervelocity impact. For this report the importance lies in the hypothesis that the nuclear dust cloud particle is approximately 20μ in diameter. Since the majority of meaningful impact data has been obtained with particles 200μ in diameter or greater, extrapolation of the data to the smaller size is necessary.

(U) Until recently it has been believed that hypervelocity impact craters obeyed a modified explosive or Hopkinson scaling law. Applied to impacts, it can be stated that if two impacts are identical in all but size the craters' dimensions will be proportional to the cube root of projectile volume, i.e., to a characteristic projectile dimension, Reference 2. This can be expressed as

$$\frac{P}{D_s} = f(v)$$

or

$$\frac{D_c}{D_s} = g(v)$$

where P is depth of penetration, D_s is a projectile dimension, D_c is crater diameter, and f and g are functions of velocity. If, as is generally the case for hypervelocity impacts of compact projectiles into metals, a hemi-spherical crater is produced, this scaling law requires the crater volume V_c to be proportional to the projectile dimension cubed.

(U) If such a scaling law does not hold true then there can exist the more complex situation:

$$\frac{P}{D_s} = f(D_s,v)$$

$$\frac{D_c}{D_s} = g(D_s,v)$$

where f and g are now functions of both projectile size and velocity. As a result, determination of scaling laws becomes more complicated. A possible explanation as to why the modified scaling law does not hold true is material strain-rate effects. The yield stress is dependent upon the rate of loading of the material; this has been experimentally verified for many plastics and certain metals, References 3 and 4.

(S) Figures 3 and 4 show experimental curves which illustrate the above mentioned size effect. Figure 3 shows penetration versus sphere diameter for impacts of aluminum and glass spheres into phenolic nylon, and glass spheres into 1100F aluminum, Reference 1. For

these data the magnitude of variation in impact velocities is not considered to be a significant factor in determining the effect of particle size on damage, and a constant velocity situation is assumed. The conditions for the curves in Figure 3 can be summarized in the following equations:

$$P(mm) = 2.37 D_s^{1.167} \quad (mm) \qquad (1)$$ Al and glass spheres → p.n. Velocity range: 6.1-7.7 km/sec

$$P(mm) = 2.42 D_s^{1.117} \quad (mm) \qquad (2)$$ Glass spheres → 1100F Al Velocity: 6.3 km/sec

Although this report is primarily concerned with impact damage to ablative materials the aluminum data are presented to emphasize the validity of the size effect. Crater dimensions in soft aluminum can be measured more accurately than in brittle, frangible ablative materials.

(S) Numerical results for the penetration of a 20μ particle into phenolic nylon from Equation (1) and the average value of $\frac{P}{D_s}$, from Equation (1a) below are listed in Table 1.

$$\frac{P}{D_s} = 2.30 \qquad (1a)$$

TABLE 1

D_s (mm)	P (mm) Eq. (1)	P (mm) Eq. (1a)
0.02	0.025	0.046

Equation (1a) will overestimate the depth of penetration by almost a factor of two. From the viewpoint of designing a protective system against micro-particle impact this would necessitate an undue weight penalty on the vehicle.

(S) Since mass loss is material density, ρ_t, times crater volume, V_c, the validity of modified explosive scaling can be examined from mass loss information. This type of scaling would require the mass loss to be proportional to D_s^3. Equations (3) and (4) which have been obtained from experimental data show the exponents to be slightly greater than three.

(S) Figure 4 shows $\frac{M_L}{n}$ or mass loss per impact versus particle size for phenolic nylon and o.t.w.r. ablatives. As with the penetration results, a constant velocity is assumed. The data have been fitted to straight lines on the log-log plot by the method of least squares. These curves are described by the following relationships:

$$\frac{M_L}{n} \text{ (Grams/impact)} = 0.047\ D_s^{3.503} \text{(mm)} \quad (3)$$ Al & glass spheres → p.n
Vel. range: 6.1-7.7 km/sec

$$\frac{M_L}{n} \text{ (Grams/impact)} = 0.052\ D_s^{3.169} \text{(mm)} \quad (4)$$ Glass spheres → o.t.w.r.
Velocity: 6.4 km/sec

The agreement between the two curves is considered good, even though the data for o.t.w.r. are limited. For a 20μ dust particle Equation (3) will give

$$\frac{M_L}{n} = 0.0525 \text{ micrograms/impact}$$

while the average value of

$$\frac{M_L}{nD_s^3} = 0.0607$$

gives

$$\frac{M_L}{n} = 0.486 \text{ micrograms/impact}$$

As with the penetration predictions, the difference between the results predicted by the two equations is substantial, a factor of 9.2.

(U) Impacts into o.t.w.r. were not compared in a similar manner due to the lack of sufficient data.

III. IMPACT DAMAGE TO VIRGIN ABLATIVE MATERIALS (U)

A. Analysis of Depth of Penetration Data (U)

(S) Previously reported data (Reference 1) shown in Figure 5 for 3.18-mm aluminum spheres impacting phenolic nylon at normal incidence show good correlation with Walsh's theoretical formula, Reference 5:

$$\frac{P}{D_s} = K\left(\frac{\rho_p}{\rho_t}\right)^{1/3}\left(\frac{v}{C_t}\right)^{0.58} \qquad (5)$$

where K is an experimentally determined constant obtained from one impact experiment or averaged from a series of experiments. Energy scaling, Reference 6, makes the exponent 0.667 (2/3) rather than 0.58. The numerical value for the constant, K = 1.20, is dependent on the strength of the impacted material and was averaged from all the impact data where the condition

$\frac{v}{C_t} > 1$ held true.

(S) Also shown in Figure 5 is a curve obtained from a linear least squares fit on log-log paper of the data for $\frac{v}{C_t} \geq 1$; where $\frac{P}{D_s}\left(\frac{\rho_t}{\rho_p}\right)^{1/3}$ was plotted as a function of $\frac{v}{C_t}$.

The intercept at log $\frac{v}{C_t} = 1$ gave the value of the constant, K, equal to 1.284 and the slope provided the value of the exponent, 0.508; the agreement with the curve obtained from Walsh's expression is obvious.

(U) As discussed in Section II, projectile size can be of importance in determining crater dimensions. The data presented in Figure 5 are from the same size projectiles and the question of size is not pertinent.

(U) Additional data have been accumulated with 3.18-mm glass spheres into virgin p.n., virgin o.t.w.r., and virgin c.p. Velocities ranged from 0.74 to 7.9 km/sec and the firings were at angles of obliquity, θ, ranging from 45° to 90°. Also shown are data from Reference 1.

(S) Depth of penetration versus impact velocity plotted in dimensionless variables is shown in Figure 6 for the impacts described above. The ordinate is

$$\frac{P}{D_s}\left(\frac{\rho_t}{\rho_p}\right)^{1/3}$$

where P and D_s have been previously defined, and ρ_t and ρ_p are target and projectile densities respectively; the abscissa is the normal component of impact velocity, v SINθ, divided by target sound speed, C_t. The penetration depth is proportional to the velocity component normal to the surface with exception of very small angles of obliquity, in the order of twenty degrees and less.

(S) Two curves are shown on the graph. These were obtained from logarithmic least squares fits of all the data and for

$\frac{v\ \mathrm{SIN}\theta}{C_t} \geq 1.$

An exponential equation of the form:

$$\frac{P}{D_s} = K\left(\frac{\rho_p}{\rho_t}\right)^{1/3}\left(\frac{v\ \mathrm{SIN}\theta}{C_t}\right)^{\alpha}$$

was chosen.

For all data: K = 1.35, α = 0.898.

For $\frac{v \, SIN\theta}{C_t} \geq 1$: $K = 1.71$, $\alpha = 0.453$.

The ablative materials can be evaluated in aggregate since they have similar pertinent physical properties: densities, sound speeds, and compressive strengths; see Table 2. The steep initial slope of the "all data" curve accounts for the 0.898 exponent. There is some indication of a transition occuring at $\frac{v \, SIN\theta}{C_t} = 1$.

The data above this value indicate that the depth of penetration is increasing at a slower rate as the velocity is increasing.

(U) A complete theoretical solution to the high-speed impact problem is dependent upon the target material's constitutive equations. These equations describe the relationships between time dependent stress and strain fields within the material. The solution would predict crater dimensions for a given impact situation and a value of K could be determined by solving the penetration equation for K. At this time the complete theoretical solution has not been successfully obtained, and experimental results are necessary to produce engineering curves for extrapolative and design purposes.

B. Analysis of Mass Loss Data (U)

(U) The amount of material removed from a thermal protection system due to hypervelocity impacts of dust particles is of primary importance for a vulnerability analysis of ballistic missiles. Tests have been conducted and correlations made of ablative material mass loss as a function of important test parameters such as impact energy, angle of incidence, etc., see Reference 1.

TABLE 2

Mechanical Properties of Ablative Materials

Materials	*O.t.w.r.	**Phenolic nylon	**Carbon phenolic
Density, gms/cc	1.55	1.19	1.49
Sound Speed, km/sec ***	3.0	2.9	3.7
Ultimate Tensile Strength, psi x 10^{-3}	1 - 5	1 - 5	15
Ult. Compressive Strength, psi x 10^{-3}	20 - 30	20 - 50	25
Tens. Modulus of Elasticity, psi x 10^{-6}	2 - 2.5	3 - 4	-
Comp. Modulus of Elasticity, psi x 10^{-6}	1.9 - 2.2	1 - 2	-

*AVCO paper, AMRAC Proceedings, Vol. VII, Part II, Nov 1-2 1962 at Philadelphia, Pa.
**GE letter of March 24, 1967, (personal communication).
***Tests made at NRL.

(U) An empirical equation to predict mass loss can be obtained in a straight forward manner if the hypothesis is accepted that the impact energy/crater volume is constant or has a weak dependence on velocity over the velocity region of interest. This has been experimentally proven for impacts into thick metallic targets, Reference 7.

(S) Since the mass loss, M_L, is the crater volume, V_C, times the target density, ρ_t, the following relationship can be derived $M_L \propto \rho_t E$

where E is the impact energy. In these tests M_L was obtained in two ways: For spheres 400μ in diameter and smaller the targets were weighed before and after the tests with a precision balance, the mass loss being the difference between the two measurements; for spheres greater than 400μ in diameter the crater volume was measured by the displacement of a known volume of fine glass beads.

(S) In Reference 1 it was determined that mass loss, M_L, for virgin ablative impacts was proportional to E SINθ for angles of incidence from 90° to 20°. This is in good agreement with Reference 8 which showed that for oblique hypervelocity impacts of steel projectiles into lead targets the "cratering efficiency" defined as a ratio of the crater volume to the projectile energy is a linear function of the sine of the angle of obliquity up to about 15°. For ablative materials the mass loss is proportional to crater volume due to the absence of crater "lips".

(S) Figure 7 is a log-log plot of M_L as a function of E SINθ for impacts of 3.18-mm glass spheres into p.n., c.p., and o.t.w.r.

at normal incidence. Data obtained during the current reporting period are shown on the graph; velocities ranged from 0.74 km/sec to 7.93 km/sec. The equation of the straight line was derived in Reference 1 from glass and aluminum impacts into the three ablatives at impact angles greater than 20°. The equation reported in Reference 1 is:

$$M_L = 0.92\ (E\ \mathrm{SIN}\theta)^{1.15} \qquad (6)$$

where M_L is in milligrams and E is in joules. Experiments at angles of incidence less than 20° do not conform to the E SINθ relationship but more closely to an E $\mathrm{SIN}^2\theta$ relationship, Reference 1; one possible explanation is that the component of velocity normal to the impact surface is appreciably lower than the target sound speed, therefore true hypervelocity impact conditions have not been achieved. In addition as the angle θ decreases, the projectile is "smeared" out along the frontal target surface, the energy per unit frontal area is smaller and less material is removed. It has been noted that for very shallow angles the entire projectile does not penetrate the target but portions of the projectile having considerable momentum travel along the surface and can have a severe damage potential.

IV. IMPACT DAMAGE TO CHARRED ABLATIVE MATERIALS (U)

(U) Although analysis of impact damage to virgin ablative materials has some importance in the dust erosion problem; primary interest is in damage to charred ablative material. During the re-entry portion of the ICBM trajectory virgin material will be exposed to impact only when the char material along the R/V is "scrubbed off" by aerodynamic shear forces or at the relatively thick stagnation point. The probability is that charred portions of the vehicle will be struck.

(U) The difficulties inherent in obtaining meaningful terminal ballistics data with virgin ablative materials are compounded with charred materials. The chars are delicate and brittle, and extreme care must be taken in handling of the specimens. The specimens were 1/2" x 1/2" x 1/4" in size and nominal char thicknesses were 1/8" and 1/16".

A. Analysis of Room Temperature Char Impact Data (U).

(U) Initial tests were made into charred phenolic nylon targets. Two hundred micron diameter glass spheres impacted specimens having nominal char thicknesses of 1/8" and 1/16". Impact angles were 90°, 45°, and 10°. Velocities were estimated from the standardized gun loading parameters when velocity measurements were unobtainable. These velocities were 6.4 km/sec ± 0.3 km/sec.

(S) Impact damage to charred phenolic nylon targets was quite severe, large sections of char were removed from the surface and it was not possible to distinguish individual impacts. Due to the severe damage inflicted on the charred phenolic nylon targets, no correlations were made of damage characteristics such as mass loss with impact parameters. The data are listed and tabulated in Appendix 1.

(U) Meaningful information has been obtained from 200 and 400μ glass sphere impacts into carbon phenolic and o.t.w.r. specimens. Targets were weighed on a precision Mettler H16 balance to the nearest 0.1 mg shortly before and after each impact test to determine mass loss.

(S) The nature of the damage made it difficult to make an exact count of hits per target. Severe cracking and front spalling of the targets is evident, see Figs. 8 & 9. The following table lists the estimated error in determining the number of hits per target:

TABLE 3

$\Delta n = 3$	for	$n \geq 15$
$\Delta n = 2$	for	$10 \leq n < 15$
$\Delta n = 1$	for	$5 \leq n < 10$
$\Delta n = 0$	for	$5 > n$

where Δn is the variation in the number of impacts, n.

(U) The experimental results are presented in terms of C_N, which is defined by the formula

$$C_N = \frac{nE}{M_L} \tag{7}$$

where E is the kinetic energy of a single particle, n is the number of particles striking the target and M_L is the target mass loss. Based on errors in evaluation of the number of impacts per target and the impact velocity, the variation in C_N, ΔC_N, is:

$$\Delta C_N = \left[\frac{\Delta n}{n} + 2\,\frac{\Delta v}{v}\right] C_N \tag{8}$$

$\Delta v = 0.3$ km/sec for $v = 6.4$ km/sec

(S) A graph of C_N in joules/gram versus angle of obliquity in degrees is shown in Figure 10. The 200μ and 400μ glass sphere data are averaged together, and it is the average values of C_N which are plotted. Since there was only a factor of two difference in ball dimensions the effect of projectile size on damage is not considered significant. Error bars whose bounds are delineated by Eq. 8 are also shown.

(S) The values of C_N for the two materials are quite close, between two and three hundred joules/gram at the 45° and 10° obliquities. At normal incidence the carbon phenolic specimens were slightly stronger with a C_N of 227 joules/gram as compared to 153 joules/gram for o.t.w.r. See Figure 10.

B. Analysis of Hot Char Impact Data (U)

(U) A limited number of shots have been made into char-layer samples of o.t.w.r. and c.p. that were being subjected to radiant heating. Phenolic nylon was not tested due to the extensive damage inflicted on the specimens and the difficulty in determining discrete impacts as discussed in Section IV A. The heating facility is described in Section I B. The flux rates, cal/cm^2- sec, on the specimens are considerably lower than those for re-entering nose cones. Surface temperatures were measured with chromel alumel thermocouples and continuously monitored on a Mosely 680 strip chart recorder. The gun was fired when the specimen surface temperature was essentially constant; this usually took several minutes.

(S) In analyzing the results of the hot char impact tests it is assumed that the material is removed by two independent mechanisms. The material is removed by gasification of the char

due to the intense heat, and by glass sphere impacts. This phenomenon can be expressed in equation form as:

$$M_L = M_{LH} + M_{LI} \qquad (9)$$

where M_L is the total mass loss, M_{LH} is the mass loss due to heating, and M_{LI} is the mass loss due to impact. Separate heating tests were made to determine M_{LH}. These tests were conducted to simulate as closely as possible the tempertaure history of the impact experiments. The results from the calibration tests are listed below in percentage of original target mass

$$M_{LH} \text{ (o.t.w.r.)} \approx 2\%$$

$$M_{LH} \text{ (c.p.)} \approx 1.6\%$$

These findings were applied to heated char impacts and these results are also shown in Figure 10. Since the tests were limited in number, each is plotted individually. The data indicate a decrease of C_N for the heated targets. It takes less energy to remove a gram of heated char material than un-heated char material. This is expected since heating will cause the material to weaken and expand. The results for the tests are in reasonable agreement with those obtained in Reference 9 for impacts at 6.1 km/sec into heated carbon phenolic at a 12.5° angle of obliquity.

V. SUMMARY AND DISCUSSION OF RESULTS (U)

(U) The acquisition of meaningful terminal ballistics data from hypervelocity impacts into virgin and charred ablative materials is a difficult task. When the projectiles are micro-particles (400μ in diameter and less) the difficulties are compounded by the necessity of keeping the targets small. However, from the investigations reported herein and in Reference 1, certain pertinent facts

about macro and micro-particle impacts into virgin and charred ablatives have been determined.

(U)The effect of projectile size on impact damage, which has been noted for aluminum targets, manifested itself in ablative material impacts. Since the primary objective of the program is to determine the damage potential of 20μ diameter dust particles onto heat shield materials, this is an item of importance, as test projectiles were never smaller than 100μ in diameter. The majority of data was obtained with projectiles 200μ in diameter and greater.

(S) Summarized in Table 4 for virgin phenolic nylon are damage parameters, depth of penetration, P, and mass loss, M_L, described in equation form in terms of sphere diameter, D_S. These formulas can be used with some degree of confidence for purposes for extrapolation.

TABLE 4

Damage Parameter		Phenolic Nylon Target Glass & Al Spheres Velocity Range: 6.1-7.7 km/sec
Penetration (mm)	=	$2.37D_S^{1.167}$(mm)
Mass Loss (grams)	=	$0.047D_S^{3.503}$(mm)

(S) It was determined that depth of penetration from 3.18-mm aluminum sphere impacts into phenolic nylon can be predicted with reasonable accuracy by an equation suggested for metal to metal impacts by Walsh, Reference 5:

$$P = K\left(\frac{\rho_p}{\rho_t}\right)^{1/3}\left(\frac{v}{C_t}\right)^{0.58} D_s$$

where K = 1.20 is a statistical average obtained from tests where $\frac{v}{C_t} \geq 1$.

(S) The effect of obliquity on penetration and mass loss of virgin ablatives was also studied, and it was concluded that both penetration and mass loss are proportional to the component of velocity normal to the impact surface for angles of obliquity between 20° and 90°. This is in good agreement with test results of hypervelocity steel projectiles into lead targets reported in Reference 8.

(S) An example will be shown of application of the results of this program. It is desired to know C_N for the impact of six interacting 20μ spheres, $\rho_p = 2.5$ gm/cm^3, onto virgin p.n., and onto room temperature and hot char-layer c.p. and o.t.w.r. targets. Impact velocity is 6.3 km/sec and θ = 10°. Lacking suitable 20μ impact test data, the following assumptions are made:

a) Projectile size and obliquity effects are independent of each other, and superposition of effects is valid.

b) The following equations having C_N as a function of projectile size and obliquity are valid for the specified encounters. These equations were derived in Reference 1.

$C_N = 378/\mathrm{SIN}^2\theta$ (joule/gram) (9) $\theta \leq 20°$, D_s = constant = 3.18 mm

$C_N = C_1 D_s^{-0.418}$ (joule/gram)(10) θ = constant = 90°.

The constant C_1 is evaluated from values of C_N obtained from test data or extrapolations of test data.

c) Available hot char-layer data at $\theta = 90°$ can be extrapolated to $\theta = 10°$ by assuming the hot char curves parallel the room-temperature char curves.

d) Damage augmentation results, Reference 1, Figure 27(b) are applicable to the stated situations.

(S) The results of the calculations are shown in Table 5 below. Appendix 2 shows detailed computations.

TABLE 5

C_N
(joules/gram)

	Without augmentation effect	With augmentation effect
Virgin p.n.	103,000	43,000
Room temperature char-layer c.p. and o.t.w.r.	780	325
Hot char-layer (1600°F) c.p. and o.t.w.r.	525	220

(U) An important unexplored aspect of the dust erosion problem is the study of the thermodynamic influences on impact damage to heated char-layer specimens. Proper thermodynamic scaling of flux rate, boundary layer thickness, etc. are necessary to create a truly realistic analog to an operational situation. The simplistic approach of de-coupling the thermodynamic and impact effects on char material removal, as used in this report, may not be realistic and this topic needs further study.

REFERENCES(U)

1. Davis, J.A. and Persechino, M.A., "Experimental Study of Small Particle Impacts Into Ablative Materials", NRL Memorandum Report 1813, August 1967. (S)

2. Hopkins, H.G. and Kolsky, H., "Mechanics of Hypervelocity Impacts of Solids", Fourth Hypervelocity Impact Symposium, Vol. I, September 1960.

3. Hopkins, H.G., "Mechanical Waves and Strain-Rate Effects in Metals", Stress Waves in Anelastic Solids, Springer Verlag, 1964.

4. Ilyushin, A. and Lensky, V., Strength of Materials, Pergamon Press, 1967.

5. Walsh, J.M. and Johnson, W.E., "On the Theory of Hypervelocity Impact", Seventh Hypervelocity Impact Symposium, Vol. II, February 1965.

6. Riney, T.D. and Heyda, J.F., "Hypervelocity Impact Calculations", Seventh Hypervelocity Impact Symposium, Vol. II, February 1965.

7. Halperson, S.M., "Comparisons Between Hydrodynamic Theory and Impact Experiments", Seventh Hypervelocity Impact Symposium, Vol. V, February 1965.

8. Bryan, G.M., "A Model of Oblique Impact", Fourth Hypervelocity Impact Symposium, Vol. III, 1960.

9. Anonymous, "R/V Material-Dust C_N at Wall Temperatures 300-3083° K", Rhodes & Bloxom Report, March 1968. (S)

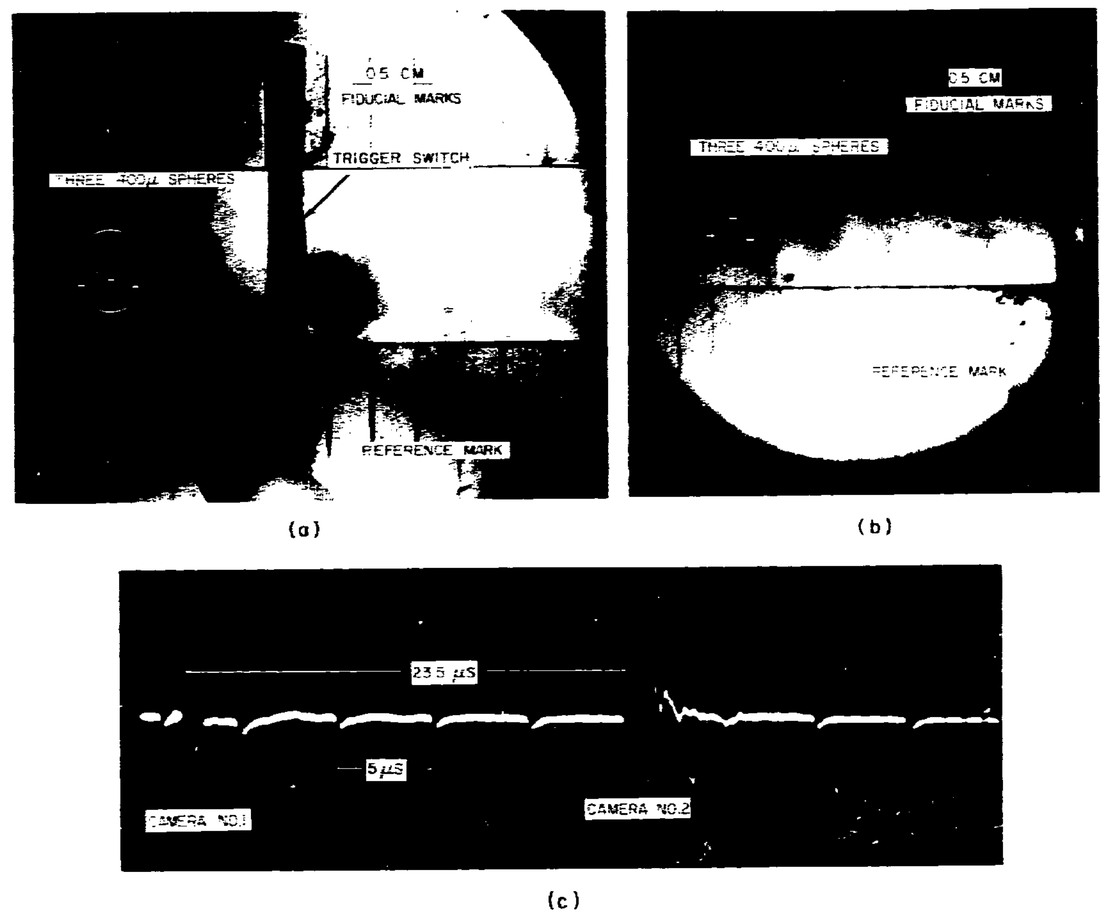

Figure 1 - Photographs and timing trace for three 400μ diameter spheres, velocity: 6.28 km/sec. (a) Camera No. 1, view of vertical plane (b) Camera No. 2, view of horizonal plane (c) Timing trace.

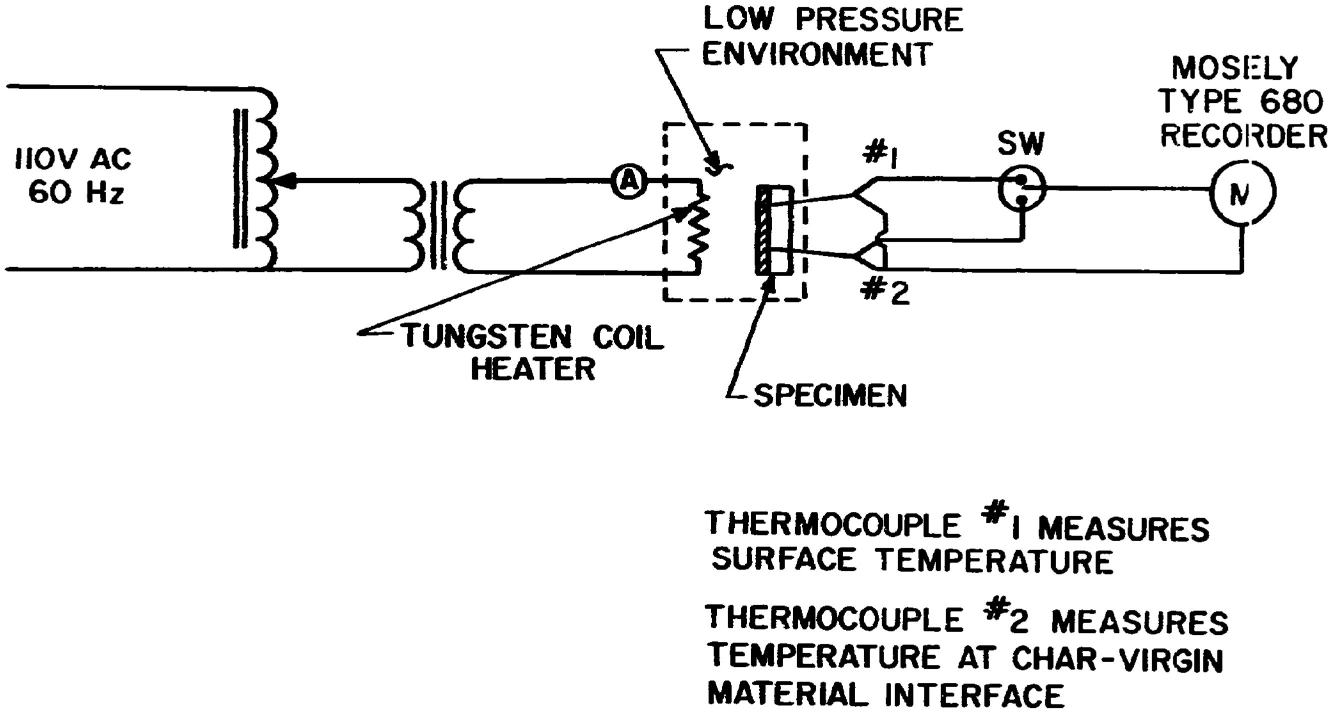

Figure 2 - Schematic for char-layer ablative specimen heating and impact tests

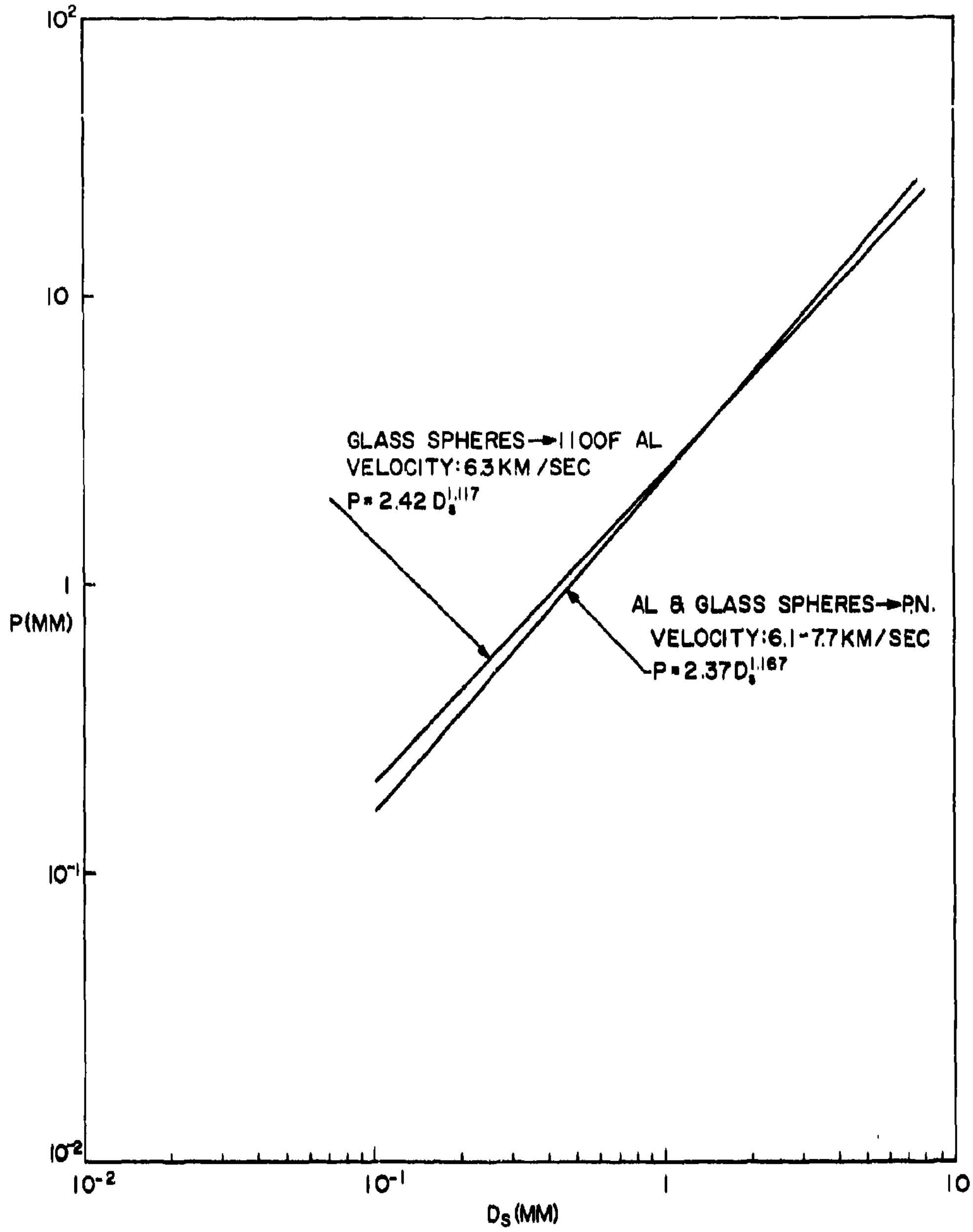

Figure 3 - Penetration versus sphere size for impacts of glass spheres into 1100F aluminum, and aluminum and glass spheres into phenolic nylon.

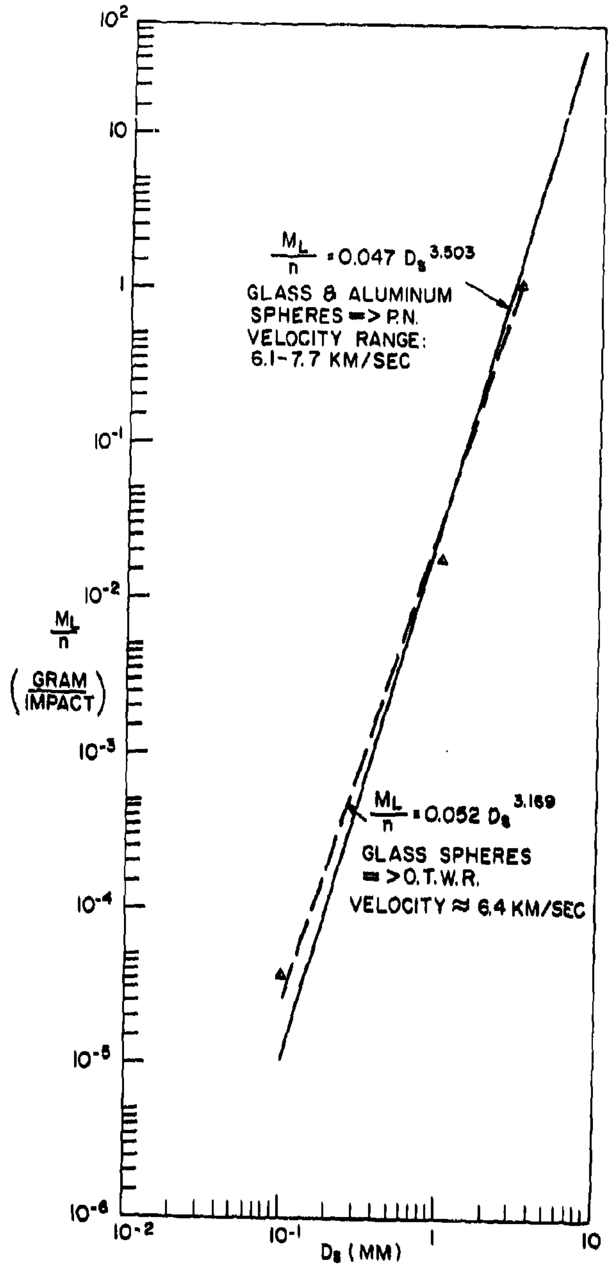

Figure 4 - Mass loss/impact versus sphere size for impacts of glass spheres into oblique tape wound refrasil, and aluminum and glass spheres into phenolic nylon.

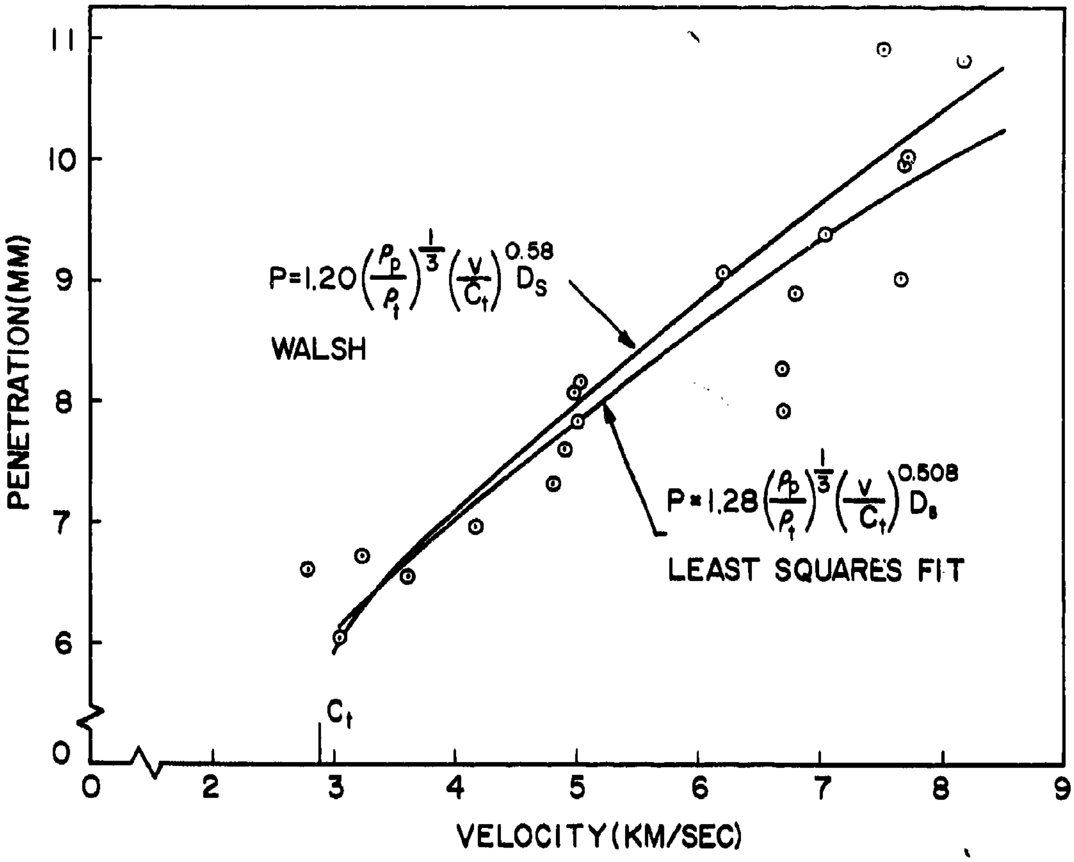

Figure 5 - Penetration versus velocity for impacts of 3.18 mm aluminum spheres into phenolic nylon at normal incidence

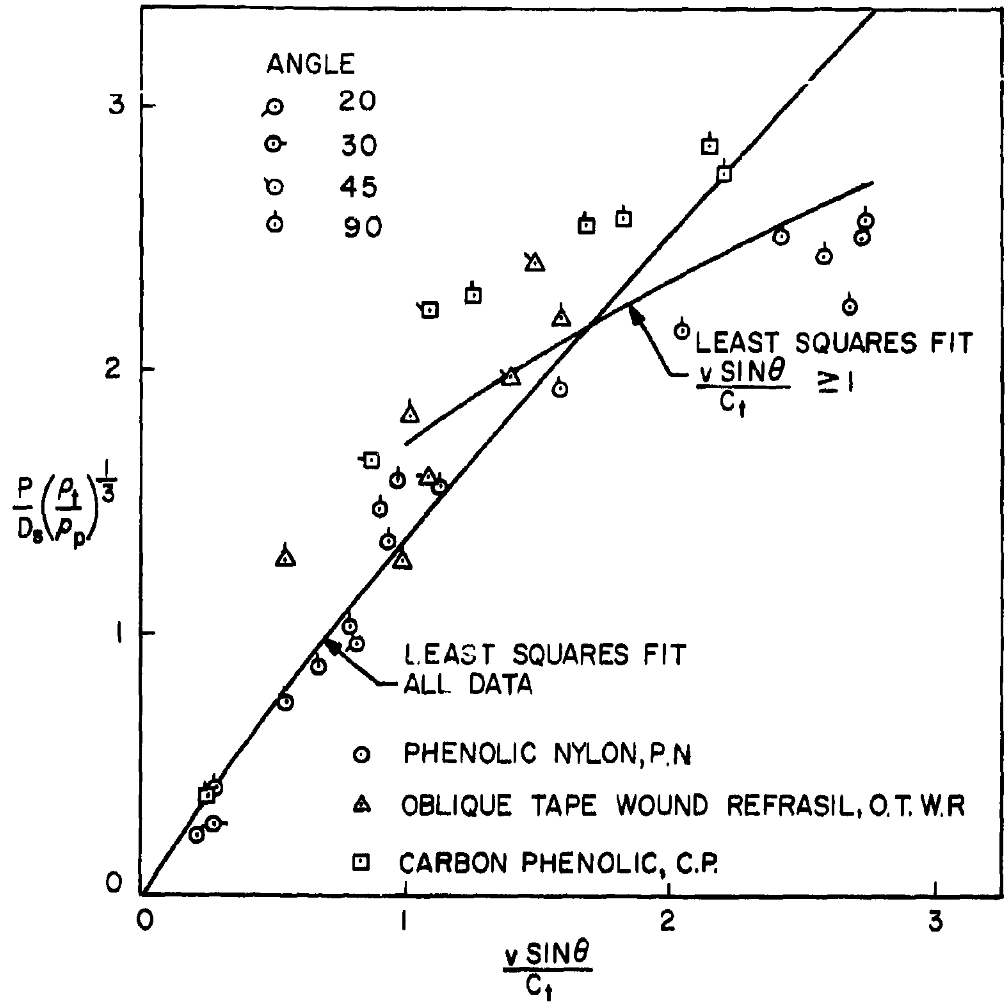

Figure 6 - Normalized depth of penetration versus normalized impact velocity for 3.18 mm glass spheres into phenolic nylon, oblique tape wound refrasil, and carbon phenolic.

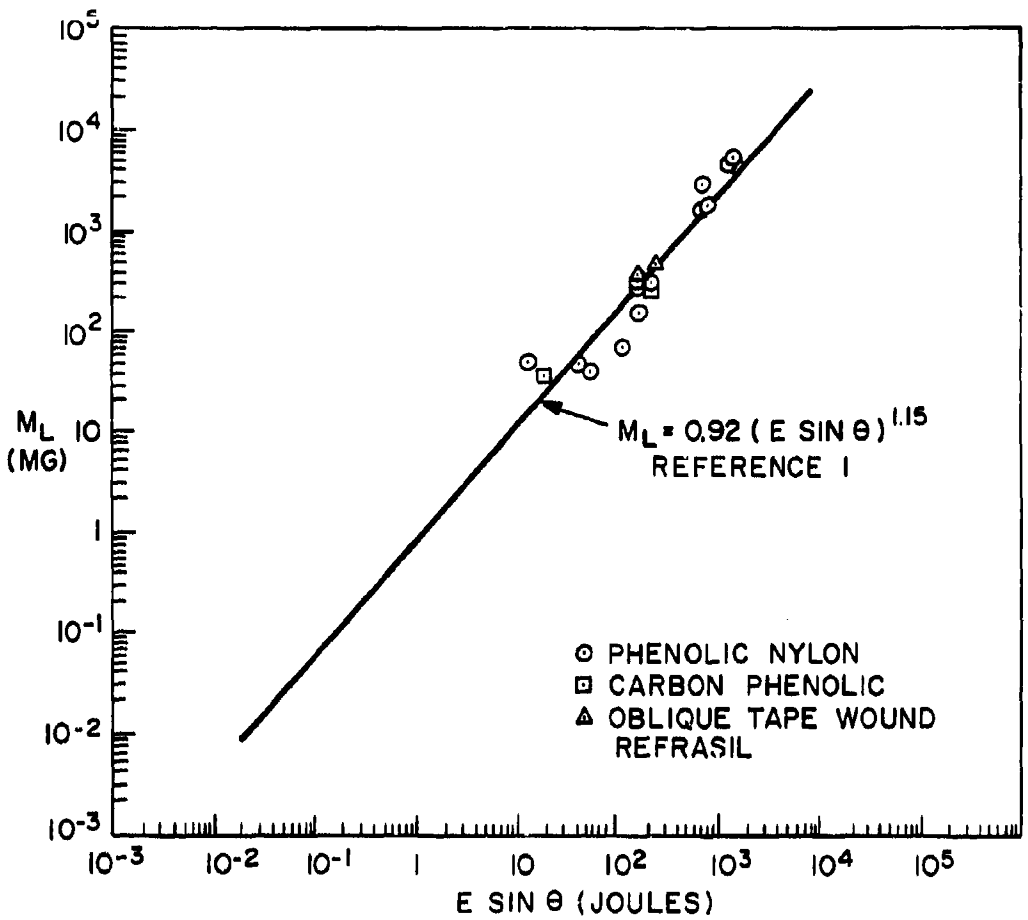

Figure 7 - Mass loss versus impact energy x Sinθ for 3.18 mm glass spheres into phenolic nylon, carbon phenolic, and oblique tape wound refrasil.

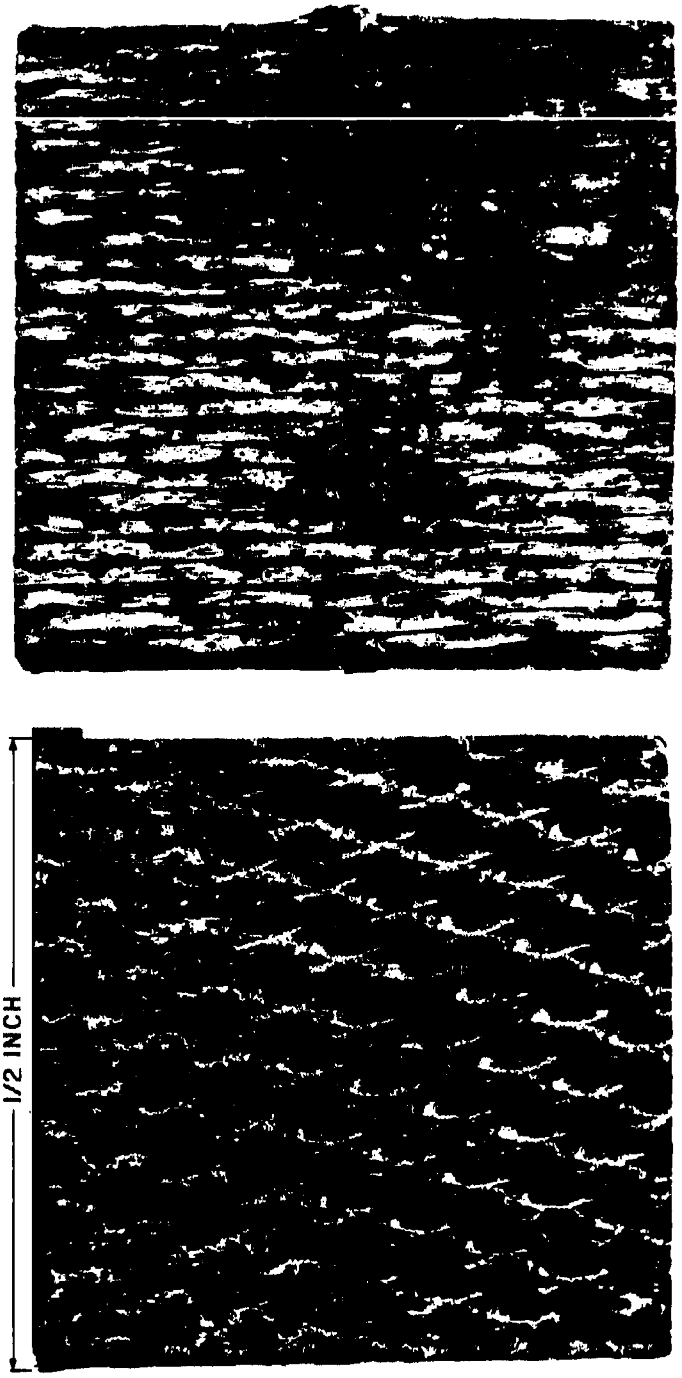

Figure 8 - Before and after photographs of 1/8 inch char-layer carbon phenolic impacted by 400 μ glass spheres at approximately 6.4 km/sec.

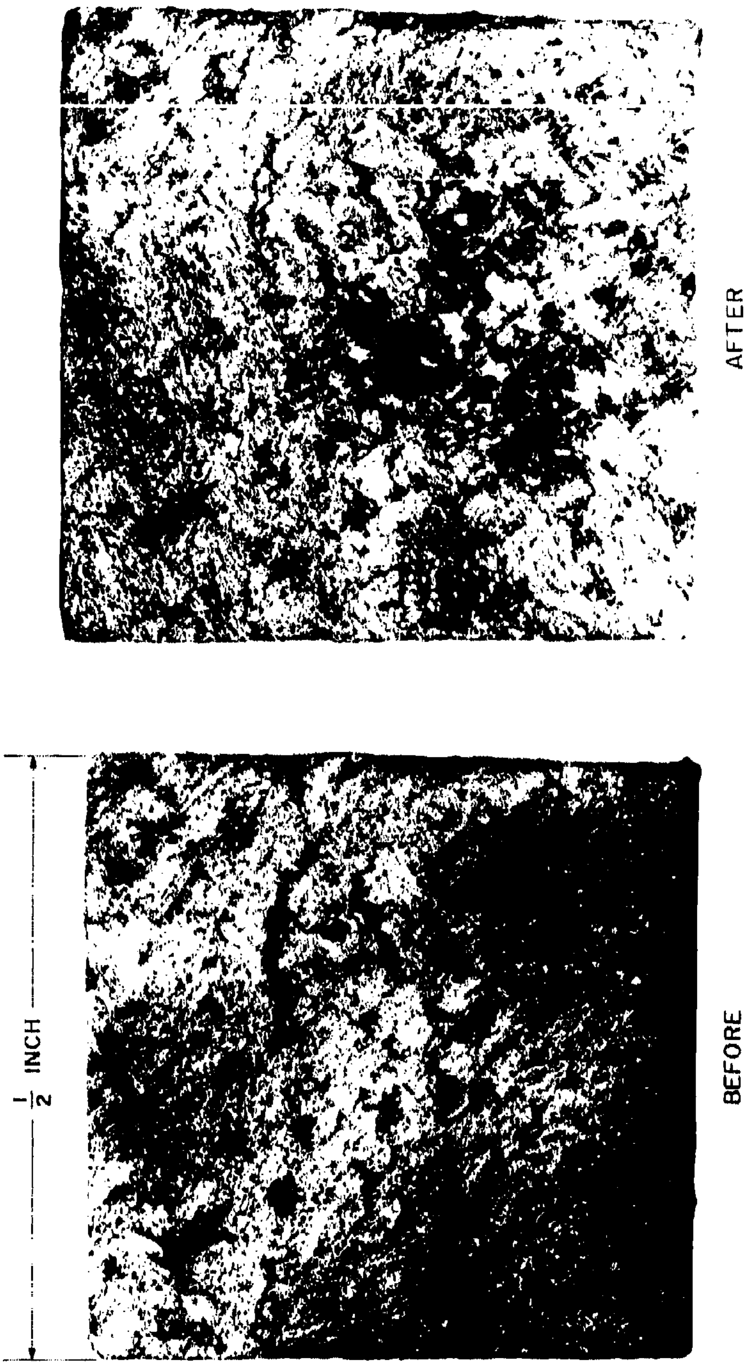

Figure 9 - Before and after photographs of 1/16 inch char-layer o.t.w.r. impacted by 200μ glass spheres at approximately 6.4 km/sec.

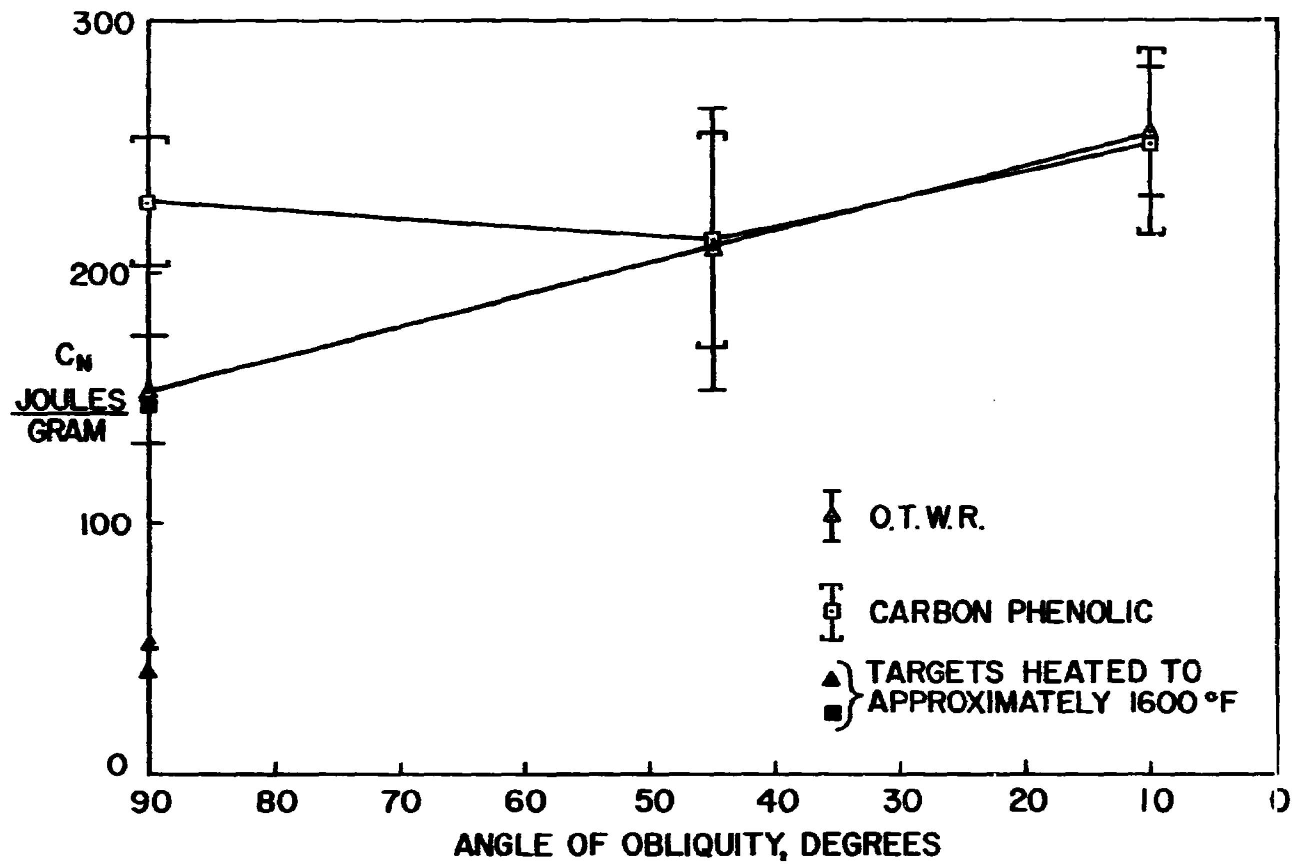

Figure 10 - C_N versus angle of obliquity for 200μ and 400μ glass sphere impacts into room temperature and heated char-layer c.p. and o.t.w.r.

APPENDIX 1

SUMMARY OF GLASS SPHERE IMPACT DATA (U)

MACRO-PARTICLE RESULTS

3.18 mm Diameter Spheres At Normal Incidence, $\theta = 90°$

PROJECTILE				TARGET			
Round No.	Mass (mg)	Velocity (km/sec)	Energy, E (joules)	Material	Pene-tration, P (mm)	Volume, Vc (cm^3)	Mass Loss, M_L (gm)**
0249	37.44	3.26	198.96	P.N.	6.20	0.26	0.31
0250	42.66	2.24	107.08	P.N.	4.06	0.06	0.07
0251	42.60	1.46	45.37	P.N.	1.91	0.04	0.048
0253	42.34	1.59	53.52	P.N.	2.92	0.03	0.036
0255	42.48	0.74	11.64	P.N.	1.52	0.04	0.048
0270	42.56	2.79	165.64	P.N.	6.32	0.12	0.14
0271	42.28	2.68	151.83	P.N.	5.41	0.28	0.33
0272	46.8	2.67	166.82	P.N.	5.94	0.24	0.29
0276	42.52	6.20	817.23	P.N.	10.05	1.45	1.72
0277	42.31	7.62*	1,227.97	P.N.	10.54	4.55	5.41
0278	42.32	7.45	1,174.38	P.N.	9.80	3.75	4.46
0279	42.10	7.62*	1,222.16	P.N.	8.61	3.90	4.64
0280	38.22	7.89	1,189.60	P.N.	10.05	4.40	5.24
0281	38.12	7.93	1,198.49	P.N.	10.31	3.75	4.46
0349	42.50	5.85*	727.18	P.N.	8.53	2.40	2.85
0350	38.16	5.93	670.85	P.N.	8.61	1.40	1.67

*Estimated from gun loading parameters.
**Obtained by multiplying V_c by ρ_t.

APPENDIX 1

SUMMARY OF GLASS SPHERE IMPACT DATA (U)

MICRO-PARTICLE RESULTS

PROJECTILE					TARGET			
Round No.	Diam., D_s (mm)	Mass (mg)	Velocity (km/sec)	Energy, E (joules)#	θ (deg)	Material	Mass Loss, M_L (gm)	No. of Impacts, (n)
0285	0.1	0.0015	6.4*	0.403	90	O.T.W.R.	$.865 \times 10^{-3}$	13
0286	0.1	0.0015	6.4*	0.465	90	O.T.W.R.	$.949 \times 10^{-3}$	15
0282	0.2	0.012	6.36	-	90	⅛" char P.N.	.009	##
0283	0.2	0.012	6.37	-	90	⅛" char P.N.	.016	##
0284	0.2	0.012	5.92	-	45	⅛" char P.N.	.028	##
0288	0.2	0.012	6.4*	-	10	⅛" char P.N.	.036	##
0289	0.2	0.012	6.4*	-	90	1/16" char P.N.	.030	##
0290	0.2	0.012	6.4*	-	90	1/16" char P.N.	.023	##
0293	0.2	0.012	6.4*	-	45	1/16" char P.N.	.034	##
0304	0.2	0.012	6.4*	-	45	1/16" char P.N.	.014	##
0306	0.2	0.012	6.4*	1.47	90	1/16" char O.T.W.R.	.010	6
0307	0.2	0.012	6.4*	0.98	90	1/16" char O.T.W.R.	.009	4
0308	0.2	0.012	6.4*	1.97	45	1/16" char O.T.W.R.	.010	8

*Estimated from gun loading parameters.
**Obtained by multiplying V_c by ρ_t.
#Total energy of balls striking target.
##Unable to determine number of impacts.

APPENDIX 1

SUMMARY OF GLASS SPHERE IMPACT DATA (U)

MICRO-PARTICLE RESULTS

PROJECTILE						TARGET		
Round No.	Diam., D_s (mm)	Mass (mg)	Velocity (km/sec)	Energy, E (joules)#	θ (deg)	Material	Mass Loss, M_L(gm)	No. of Impacts, (n)
0309	0.2	0.012	6.4*	1.97	45	1/16"char O.T.W.R.	.085	8
0312	0.2	0.012	6.4*	0.246	10	1/16"char O.T.W.R.	.009	1
0313	0.2	0.012	6.4*	3.69	90	1/16"char C.P.	.011	15
0314	0.2	0.012	6.4*	4.18	90	1/16"char C.P.	.017	17
0315	0.2	0.012	6.4*	2.21	45	1/16"char C.P	.013	9
0316	0.2	0.012	6.4*	2.46	45	1/16"char C.P.	.011	10
0318	0.2	0.012	6.4*	1.72	10	1/16"char C.P.	.015	7
0323	0.4	0.087	6.4*	1.78	90	1/16"char O.T.W.R.	.011	1
0325	0.4	0.087	6.4*	1.78	10	1/16"char O.T.W.R.	.018	1
0327	0.4	0.087	6.71	5.88	90	1/8" char C.P.	.042	3
0328	0.4	0.087	6.49	1.83	10	1/8" char C.P.	.005	1
0332	0.4	0.087	6.4*	3.56	90	1/8" char O.T.W.R.	.017	2

*Estimated from gun loading parameters.
**Obtained by multiplying V_c by ρ_t.
#Total energy of balls striking target.
##Unable to determine number of impacts.

APPENDIX 1

SUMMARY OF GLASS SPHERE IMPACT DATA (U)

MICRO-PARTICLE RESULTS

	PROJECTILE					TARGET		
Round No.	Diam., D_s (mm)	Mass (mg)	Velocity (km/sec)	Energy, E (Joules)#	θ (deg)	Material	Mass Loss M_L (gm)	No. of Impacts, (n)
0333	0.4	0.087	6.4*	3.56	90	⅛" char O.T.W.R.	.018	2
0340	0.4	0.087	6.4*	8.90	45	1/16"char C.P.	.033	5
0341	0.4	0.087	6.4*	7.12	45	1/16"char C.P.	.040	4
			Targets Heated to Approximately 1600°F.					
0319	0.2	0.012	6.4*	1.72	90	1/16"char O.T.W.R.	.062	7
0320	0.2	0.012	6.4*	1.48	90	1/16"char C.P.	.032	6
0344	0.4	0.087	6.4*	3.56	90	⅛" char O.T.W.R.	.071	2

*Estimated from gun loading parameters.
**Obtained by multiplying V_c by ρ_t.
#Total energy of balls striking target.
##Unable to determine number of impacts.

APPENDIX 2

(U) Shown below are the essential computations for the figures presented in Table 5.

(S) C_N for virgin p.n. is evaluated from Eq. (9) for $\theta = 10°$. This gives $C_N = 12{,}500$ joules/gm for 3.18 mm spheres. Using this value of C_N in Eq. (10) and solving for C_1 gives Eq. (10a),

$$C_N = 20{,}230\ D_s^{-0.418} \tag{10a}$$

for $D_s = 20\mu = 0.02$ mm, Eq. (10a) gives $C_N = 103{,}000$ joules/gm.

(S) For room-temperature char c.p. and o.t.w.r. at $\theta = 10°$, an average C_N is 250 joules/gm, see Figure 10. Equation (10) is evaluated for an average particle size of 300μ to determine C_1. This leads to

$$C_N = 152\ D_s^{-0.418} \tag{10b}$$

For a 20μ sphere Eq. (10b) gives $C_N = 775$ joules/gm.

(S) For hot char-layer c.p. and o.t.w.r. the same procedure was used to determine C_N as for room-temperature char. The only difference was that an average C_N was obtained from extrapolating data at $\theta = 90°$ to $\theta = 10°$ by assuming the hot char curves parallel the room-temperature char curves. These techniques will give an average C_N for 300μ sphere equal to 160 joules/gm and $C_N = 525$ joules/gm for 20μ spheres.

(S) For the effect of augmentation, Figure 27(b), Reference 1 provides a damage enhancement value of 2.4 for six interacting spheres. Hence all C_Ns are divided by this number to provide values for the hypothesized encounter. Values for un-augmented and augmented C_N are shown in Table 5.

SECRET

Security Classification

DOCUMENT CONTROL DATA - R & D	
(Security classification of title, body of abstract and indexing annotation must be entered when the overall report is classified)	
1. ORIGINATING ACTIVITY (Corporate author) Naval Research Laboratory Washington, D.C. 20390	2a. REPORT SECURITY CLASSIFICATION SECRET 2b. GROUP 3

3. REPORT TITLE

CONTINUATION OF EXPERIMENTAL STUDY OF SMALL PARTICLE IMPACTS INTO ABLATIVE MATERIALS

4. DESCRIPTIVE NOTES (Type of report and inclusive dates)
A Summary Report; this is the final report on this problem.

5. AUTHOR(S) (First name, middle initial, last name)

Stanley M. Halperson

6. REPORT DATE	7a. TOTAL NO. OF PAGES	7b. NO. OF REFS
July 1968	44	9
8a. CONTRACT OR GRANT NO. NRL Problem F04-11A b. PROJECT NO. ARPA Order No. 149, Amendment No. 11 c. Program Code 6E30, ARPA Order No. 149, Amendment No. 12, Program d. Code 7E30.	9a. ORIGINATOR'S REPORT NUMBER(S) 9b. OTHER REPORT NO(S) (Any other numbers that may be assigned this report)	

10. DISTRIBUTION STATEMENT In addition to security requirements which apply to this document and must be met, it may be further distributed by the holder only with specific prior approval of the Director, Naval Research Laboratory, Washington, D.C. 20390.

11. SUPPLEMENTARY NOTES	12. SPONSORING MILITARY ACTIVITY
	Dept. of Defense Advanced Research Projects Agency Washington, D.C. 20301

13. ABSTRACT

SECRET

(U) This report is a continuation of the work described in NRL Memorandum Report 1813, entitled "Experimental Study of Small Particle Impacts into Ablative Materials".

(S) Utilizing the light-gas gun, impact tests with glass spheres from 3.18 mm to 100μ in diameter were made into three ablatives; phenolic nylon, carbon phenolic, and oblique tape wound refrasil. Velocities ranged from 0.74 to 7.9 km/sec and angles of obliquities ranged from 10° to 90°.

(S) It was established that modified explosive scaling does not hold true for hypervelocity impacts into ablatives, and dimensionless damage parameter such as penetration/projectile size are dependent on both velocity and projectile dimension rather than on velocity alone.

(S) Penetration measurements of virgin phenolic nylon targets impacted by 3.18-mm aluminum spheres showed good correlation with the theoretical formula of Walsh. It was also determined that for obliquity tests where the normal velocity component/target sound speed ≥ 1, the mass loss and depth of penetration are proportional to the normal velocity component for angles of obliquity down to twenty degrees.

DD FORM 1 NOV 65 1473 (PAGE 1)

S/N 0101-807-6801

SECRET

Security Classification

14. KEY WORDS	LINK A ROLE	LINK A WT	LINK B ROLE	LINK B WT	LINK C ROLE	LINK C WT
Small particle impact						
Glass and aluminum projectiles						
Ablative materials						
Ballistic missile						

(S) Impact experiments were made with 1/2" x 1/2" x 1/4" char-layer specimens of carbon phenolic and oblique tape wound refrasil at room temperature and elevated temperatures, at normal incidence, and obliquities of 45° and 10°. Specimen mass loss was measured, and it was ascertained that for room temperature tests C_N (impact energy/mass loss) tends to increase slightly with decreasing angles of obliquity. Experiments where char-layer surface temperatures were raised to approximately 1600° F showed an expected decrease in C_N.

Naval Research Laboratory
Technical Library
Research Reports Section

DATE: November 21, 2002

FROM: Mary Templeman, Code 5227

TO: **Code 6300 Dr Gubser**

CC: Tina Smallwood, Code 1221.1 ts/11/6/03

SUBJ: Review of NRL Reports

Dear Sir/Madam:

Please review NRL Memo Reports 1760, 1541 and 1927 for:

- ☑ Possible Distribution Statement
- ☑ Possible Change in Classification

Thank you,

Mary Templeman

Mary Templeman
(202)767-3425
maryt@library.nrl.navy.mil

The subject report can be:

- ☒ Changed to Distribution A (Unlimited)
- ☒ Changed to Classification unclassified
- ☐ Other:

D W Gubser 1/2/03

Signature Date

-- 1 OF 1
- 1 - AD NUMBER: 394828
-- 2 - FIELDS AND GROUPS: 11/4, 13/1
-- 3 - ENTRY CLASSIFICATION: UNCLASSIFIED
-- 5 - CORPORATE AUTHOR: NAVAL RESEARCH LAB WASHINGTON D C
-- 6 - UNCLASSIFIED TITLE: CONTINUATION OF EXPERIMENTAL STUDY OF SMALL
-- PARTICLE IMPACTS INTO ABLATIVE MATERIALS.
-- 8 - TITLE CLASSIFICATION: UNCLASSIFIED
-- 9 - DESCRIPTIVE NOTE: FINAL REPT.,
--10 - PERSONAL AUTHORS: HALPERSON,STANLEY M. ;
--11 - REPORT DATE: JUL 1968
--12 - PAGINATION: 44P MEDIA COST: $ 7.00 PRICE CODE: AA
--14 - REPORT NUMBER: NRL-MR-1927
--15 - CONTRACT NUMBER: ARPA ORDER-149-11, ARPA ORDER-149-12
--16 - PROJECT NUMBER: NRL-F04-11A
--20 - REPORT CLASSIFICATION: CONFIDENTIAL
--22 - LIMITATIONS (ALPHA): DISTRIBUTION: CONTROLLED: ALL REQUESTS TO
-- DIRECTOR, NAVAL RESEARCH LAB., WASHINGTON, D. C. 20390.
--23 - DESCRIPTORS: (*HEAT SHIELDS, IMPACT TESTS), (*IMPACT TESTS,
-- COMPOSITE MATERIALS), GLASS TEXTILES, DUST, PENETRATION, VELOCITY,
-- PARTICLE SIZE, EROSION, DENSITY, THICKNESS, FIRING TESTS(ORDNANCE)
--24 - DESCRIPTOR CLASSIFICATION: UNCLASSIFIED
--29 - INITIAL INVENTORY: 20

--32 - REGRADE CATEGORY: C
--33 - LIMITATION CODES: 5
--34 - SOURCE SERIES: F
--35 - SOURCE CODE: 251950
--36 - ITEM LOCATION: DTIC
--38 - DECLASSIFICATION DATE: OADR
--40 - GEOPOLITICAL CODE: 1100
--41 - TYPE CODE: N
--43 - IAC DOCUMENT TYPE: